Medical Image Analysis

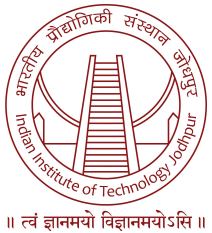

Jayant Mahawar
PhD Scholar
Department of Computer Science & Engineering

X-ray Image Analysis

X-ray Images

Wrist X-ray

Spine X-ray

Pediatric X-ray

Abdominal X-ray

* https://vindr.ai/datasets/bodypartxr

X-ray Images

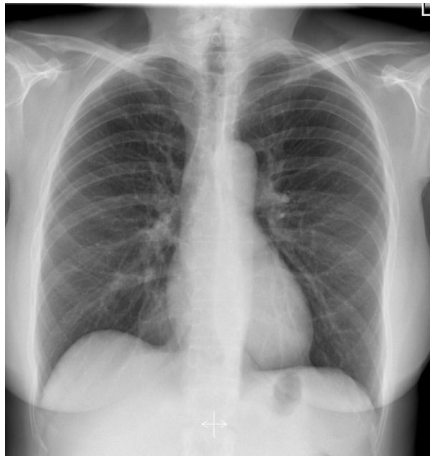

Posteroanterior (PA) view

Anteroposterior (AP) supine view

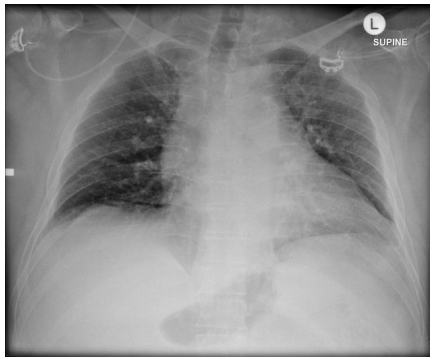

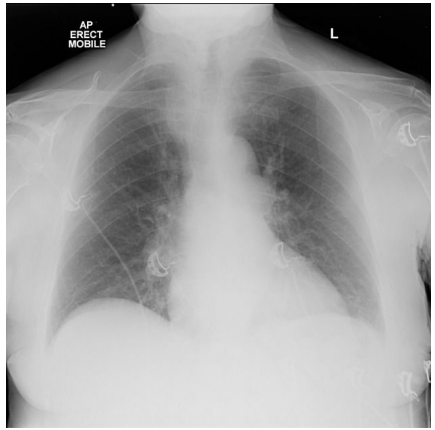

Anteroposterior (AP) erect view

Lateral view

* https://doi.org/10.53347/rID-14511

Spine X-ray - Osteophytes

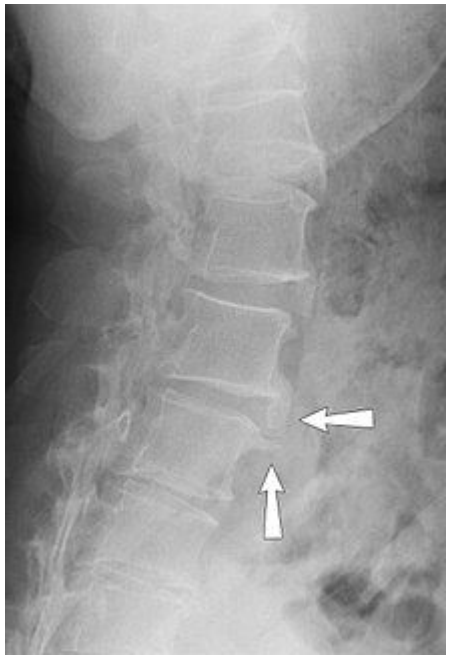

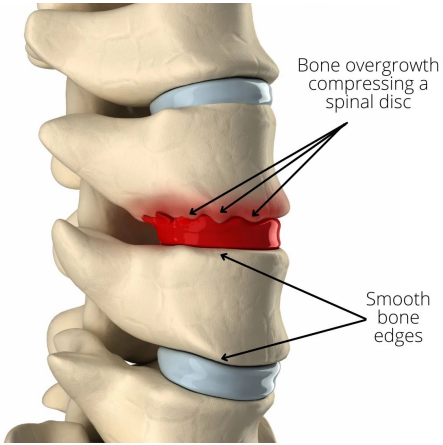

* https://www.spinalbackrack.com/what-is-a-bone-spur/

Spine X-ray - Disc Space Narrowing

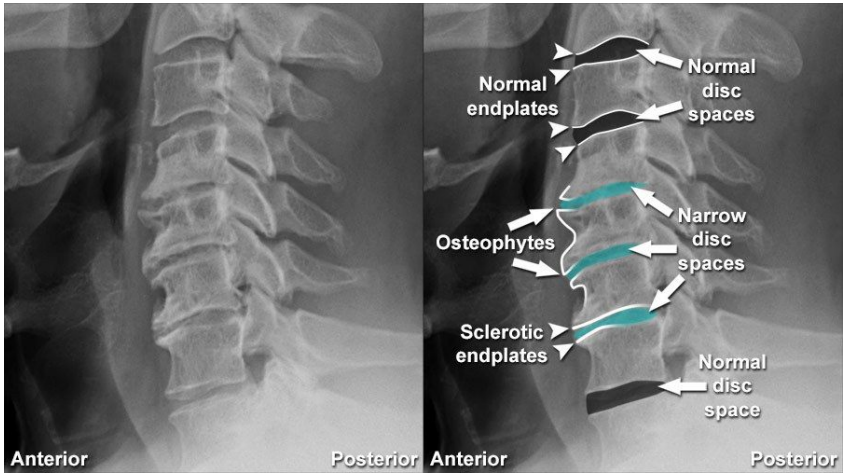

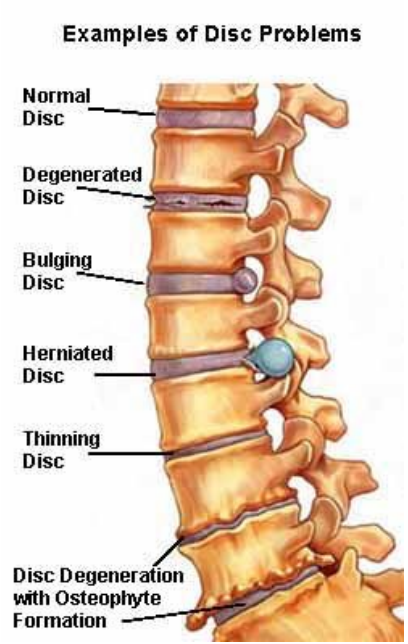

* https://www.radiologymasterclass.co.uk/tutorials/musculoskeletal/imaging-joints-bones/degenerative-disc-disease

Spine X-ray - Foraminal Stenosis

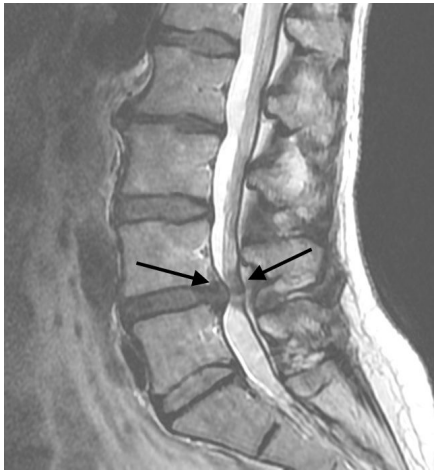

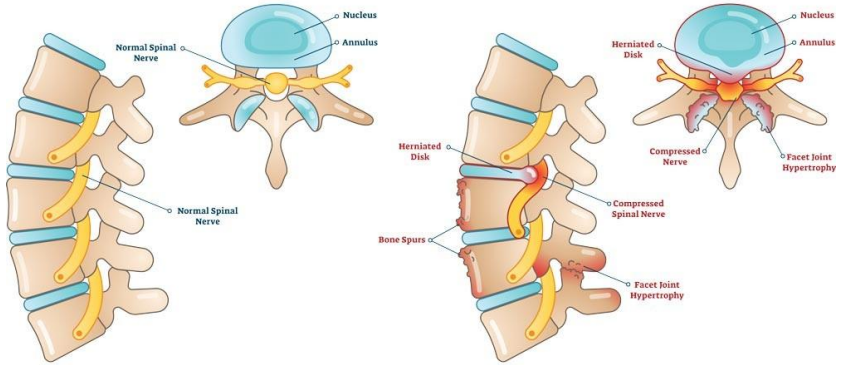

* https://texasspinecare.com/conditions/foraminal-stenosis/

AC-Faster R-CNN

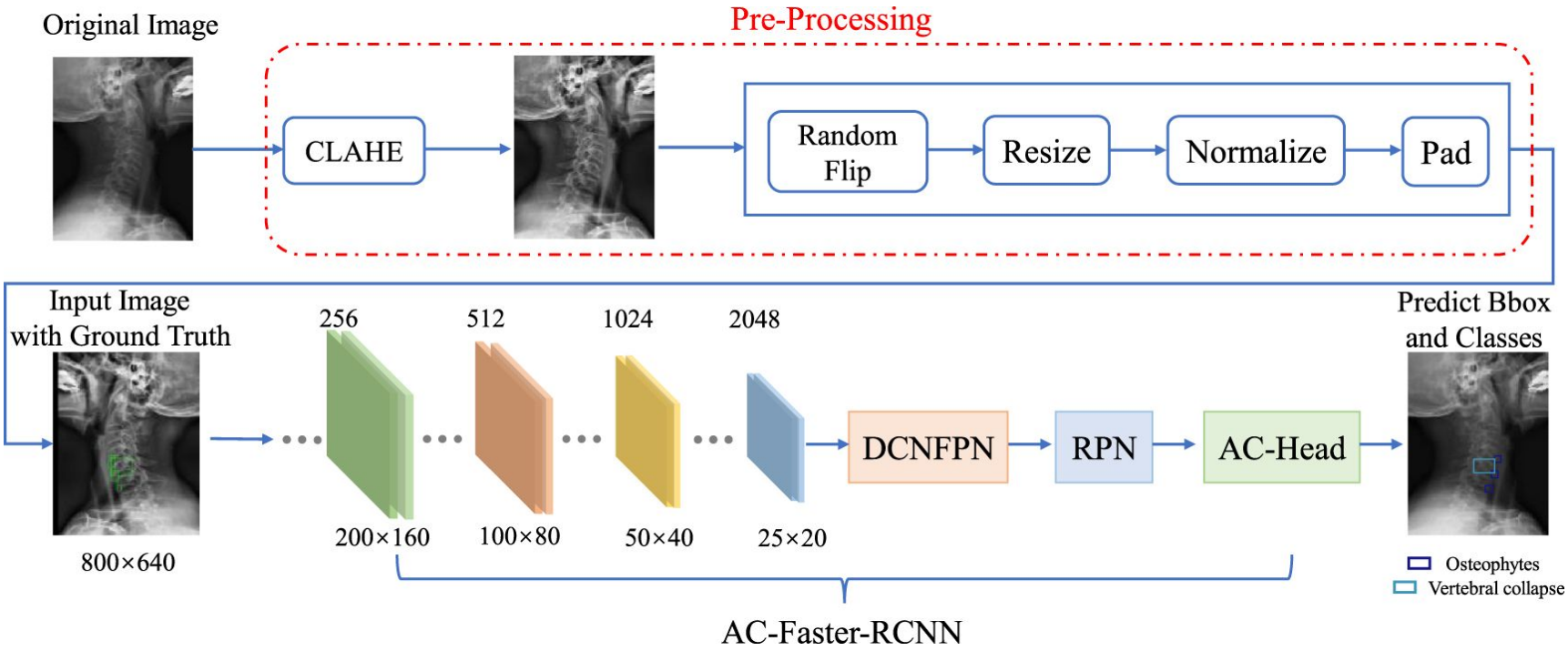

* https://doi.org/10.1088/1361-6560/acf7a8

AC-Faster R-CNN - Deformable Convolution

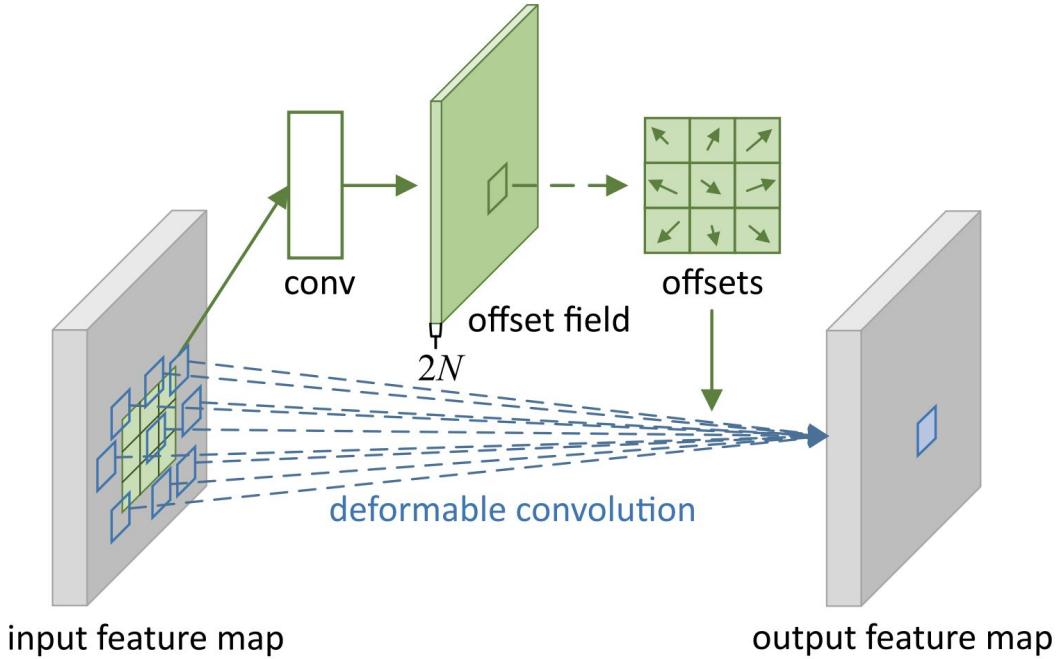

* https://doi.org/10.1088/1361-6560/acf7a8

AC-Faster R-CNN - AC- Head

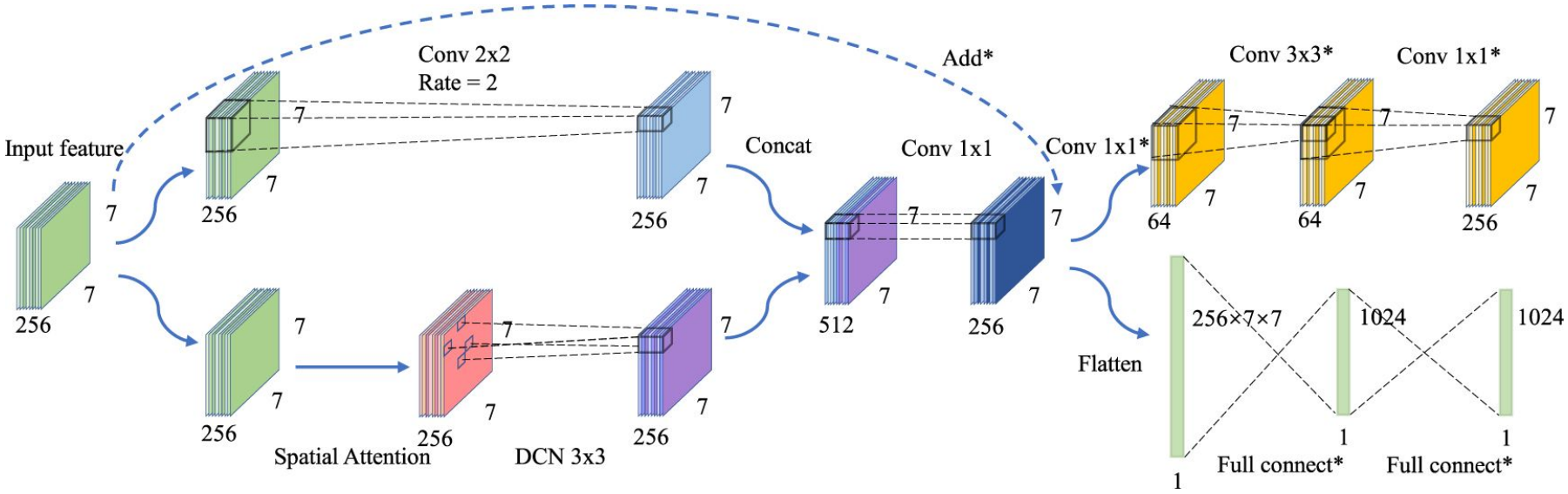

* https://doi.org/10.1088/1361-6560/acf7a8

AC-Faster R-CNN - Spatial Attention

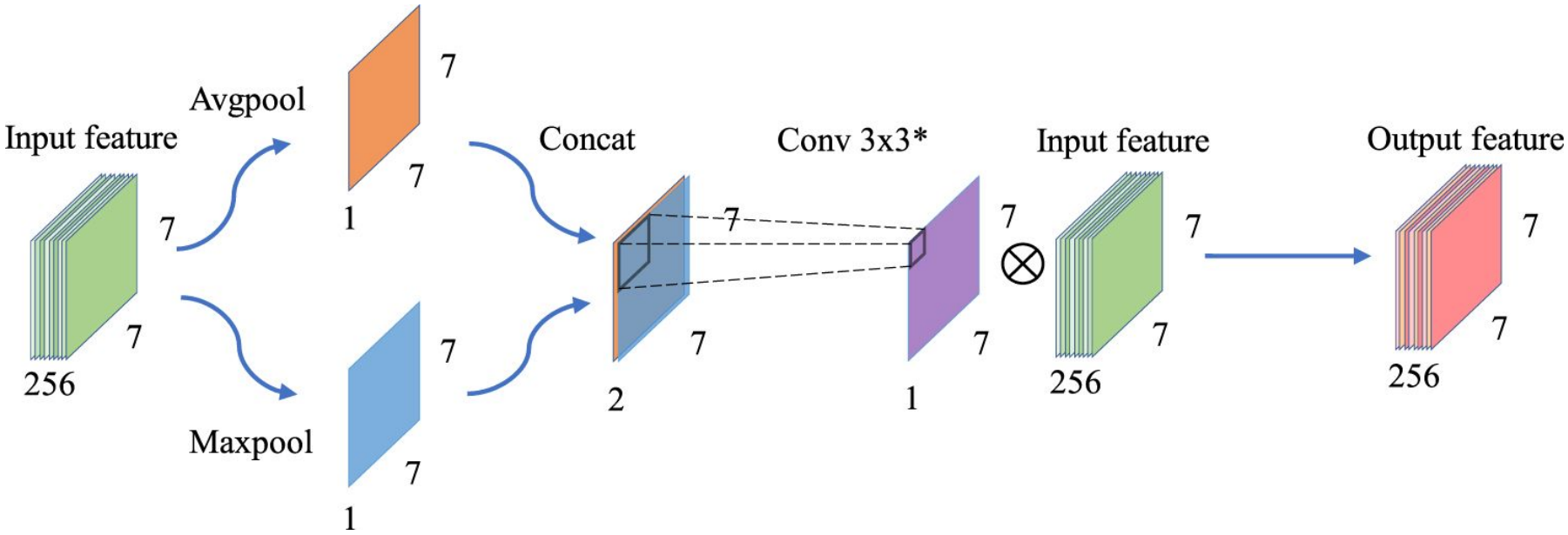

* https://doi.org/10.1088/1361-6560/acf7a8

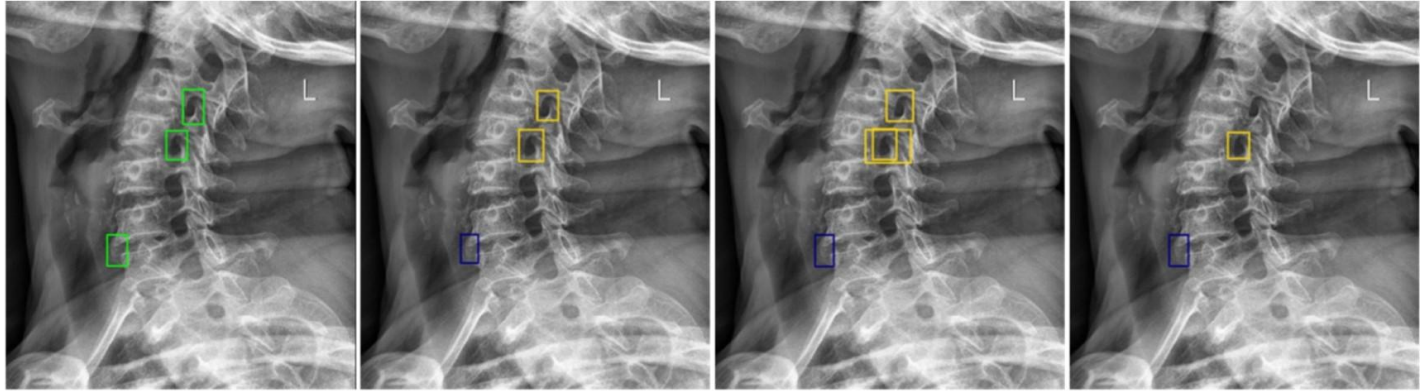

Ground Truth: 3 objects | AC-Faster-RCNN: 3 TP | Faster R-CNN: 3 TP, 1FP | Sparse R-CNN: 2 TP, 1 FN

(a) Detection results of three models on X-ray image containing Foraminal steosis and Osteophytes

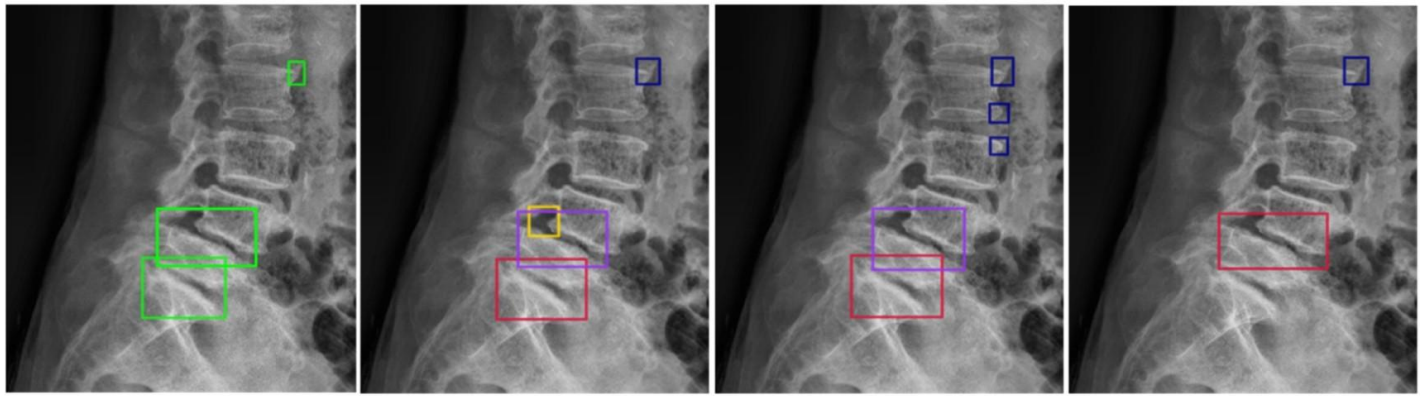

Ground Truth: 3 objects | AC-Faster-RCNN: 3 TP, 1FP | Faster R-CNN: 3 TP, 2FP | Sparse R-CNN: 1 TP ,1 FP ,1 FN

(b) Detection results of three models on X-ray image containing Spondylolysthesis, Disc space narrowing and Osteophytes

* https://doi.org/10.1088/1361-6560/acf7a8

Chest X-ray Datasets

- Large-Scale Datasets
  - NIH
  - Chexpert
- Contains Images, Text Report, Bounding Box annotations, etc.
- Erroneous labelling
- Inconsistency across datasets
- Small-Scale Datasets
  - JSRT
  - Pneumonia dataset
- Mostly contains data from 2-3 classes

Pediatric X-ray - Pediatric Lung Disorders

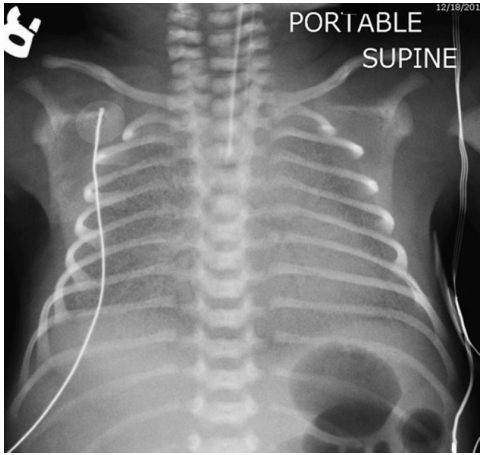

Surfactant Deficiency Syndrome

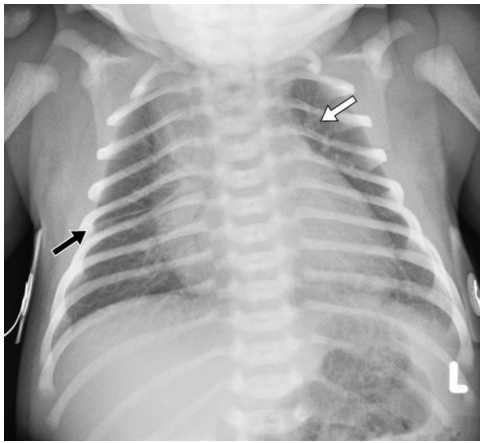

Transient Tachypnea

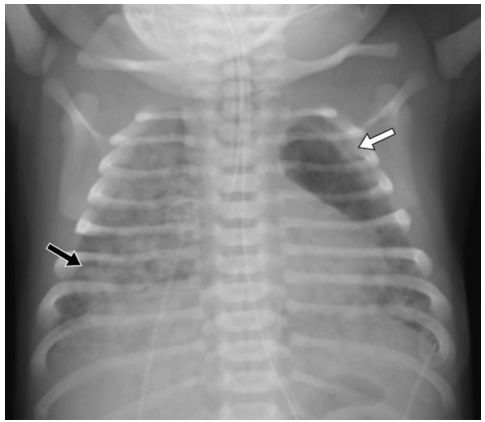

Meconium Aspiration

* https://www.ncbi.nlm.nih.gov/books/NBK553873/

Pediatric X-ray - Large Airway Disorders

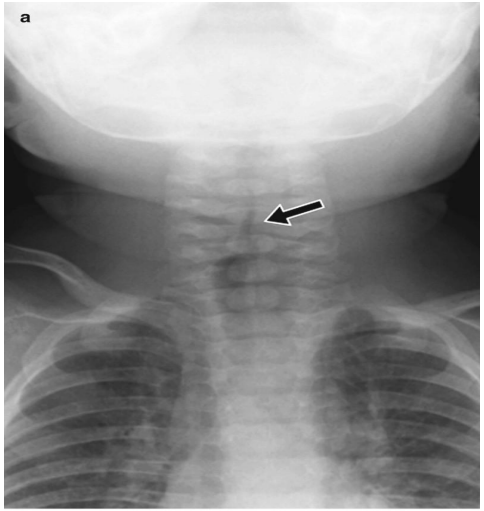

Subglottic Hemangioma

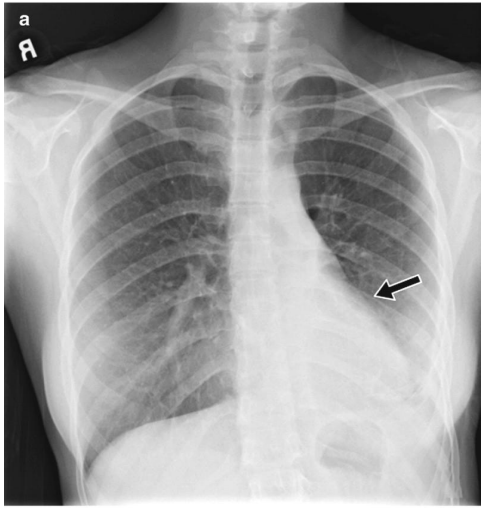

Endobronchial Carcinoid

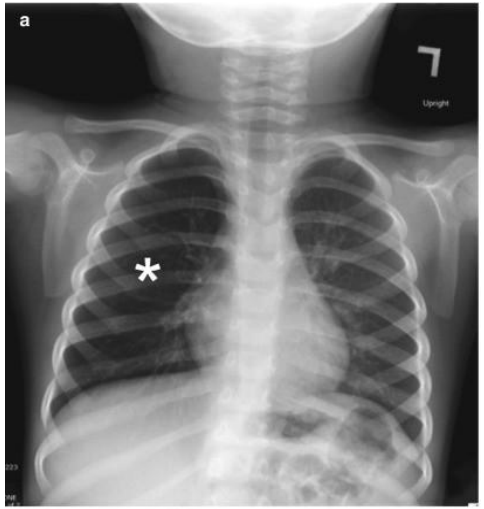

Foreign Body Aspiration

* https://www.ncbi.nlm.nih.gov/books/NBK553873/

Pediatric X-ray Analysis - DL model

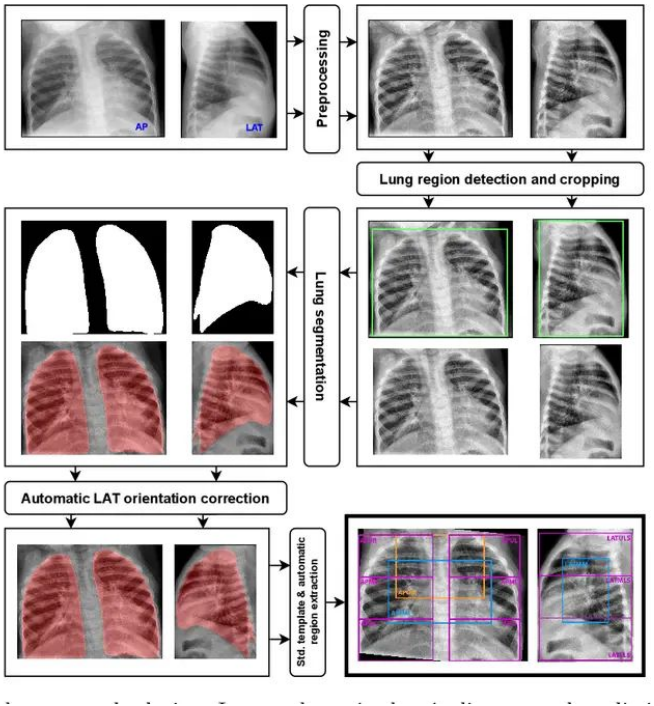

* https://arxiv.org/pdf/2301.13786v1.pdf

Chest X-ray Analysis - Bone Suppression

$$I_{\text{soft}_C}(x,y) = I(x,y) - I_{\text{bone}_C}(x,y).$$

$$T_C : (x,y) \mapsto (s,t)$$

$$T_C^{-1} : (s,t) \mapsto (x,y)$$

* https://link.springer.com/article/10.1007/s11548-015-1278-y

Chest X-ray Analysis - Bone Suppression

$$I_{st_C}(s,t) = I\left(T_C^{-1}(s,t)\right)$$

$$I_{d_C}(s,t) = \partial s I_{st_C}(s,t)$$

$$I_{r_C}(s,t) = \int_{s_0}^{s} I_{s_C} I(i,t)\, di + I_{st_C}(s_0,t).$$

* https://link.springer.com/article/10.1007/s11548-015-1278-y

Chest X-ray Analysis - Bone Suppression

$$I^{i}_{r_C}(s,t) = I_{r_C}(s,t) + \frac{I_{r_C}(\mathbf{p_c}) - I_{r_C}(\mathbf{p_i})}{2} \times \left(1 - \frac{s - c(t)}{(s_{\max} - c(t))}\right)$$

$$I_{\text{bone}_C}(x,y) = \max\left(I_{r_C}\left(T_C(x,y)\right), 0\right).$$

* https://link.springer.com/article/10.1007/s11548-015-1278-y

Chest X-ray Analysis - Bone Suppression

* https://link.springer.com/article/10.1007/s11548-015-1278-y

Chest X-ray Analysis - Bone Suppression

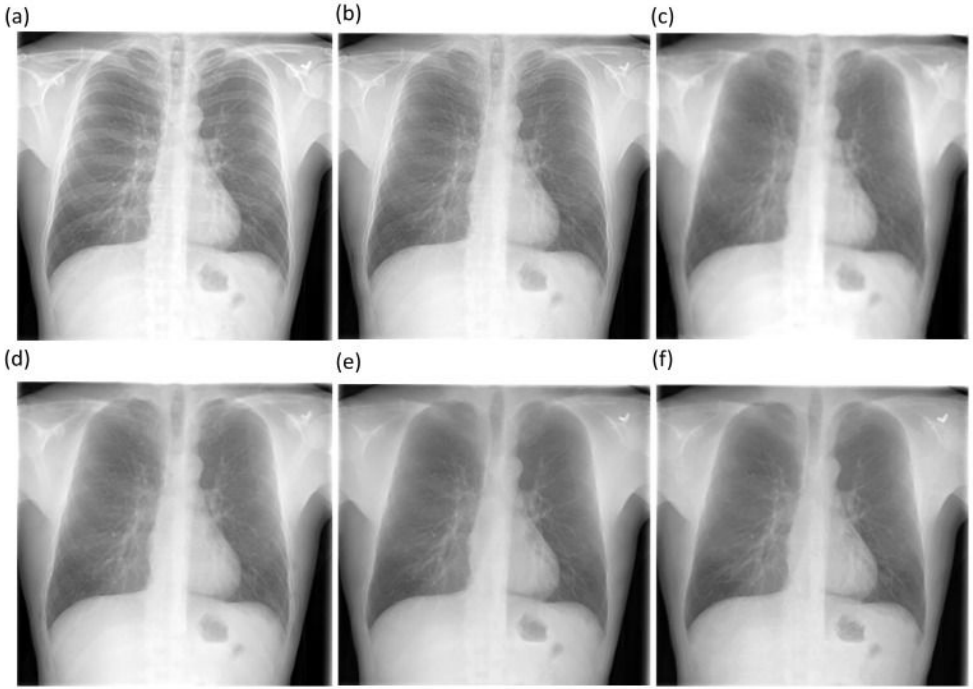

Fig. Bone-suppressed CXR images predicted by the proposed models using a CXR sample from the cross-institutional NIH–CC DES test set. (a) Original CXR; (b) AE–BS model; (c) ConvNet–BS model; (d) RL–BS model; (e) ResNet–BS model; and (f) Ground truth.

* https://www.ncbi.nlm.nih.gov/pmc/articles/PMC8151767/

Lung field Segmentation - Active Shape Model

- Training Phase
  - control points
  - scaling and alignment
- Shape Modeling
  - build a statistical shape model
  - Can use Principal Component Analysis

* https://doi.org/10.1007/978-3-642-15711-0_77

Lung field Segmentation - Active Shape Model

- Image Analysis
  - iteratively refines the model's shape
  - Energy function includes terms for shape regularization
- Optimization
  - Converges to produce segmented outline or boundary of the object of interest.

* https://doi.org/10.1007/978-3-642-15711-0_77

Lung field Segmentation - Intensity-based Model

$$H(x) = \sum_{y=1}^{N} f(x,y)$$

$$V_r(y) = \sum_{x=x_r}^{x_c} f(x,y)$$

$$V_l(y) = \sum_{x=x_{c+1}}^{x_l} f(x,y)$$

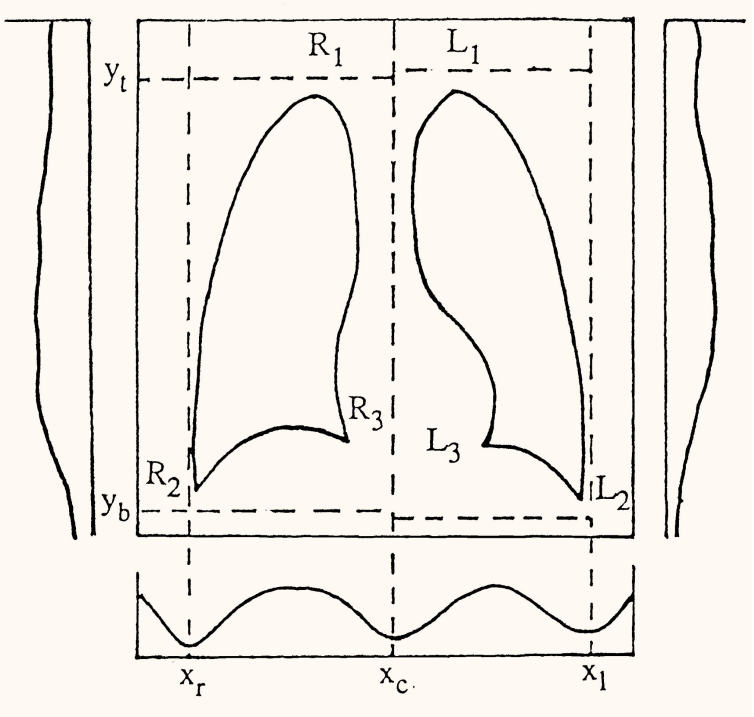

* https://ui.adsabs.harvard.edu/link_gateway/1988SPIE.1001..261C/doi:10.1117/12.968961

Lung field Segmentation - Intensity-based Model

$$p(G_i) = \frac{HI(G_i)}{A}$$

$$M = \sum_{i=1}^{N} G_i \, p(G_i)$$

$$M_1 = \frac{\sum_{i=1}^{G} G_i \, p(G_i)}{\sum_{i=1}^{G} p(G_i)} \qquad M_2 = \frac{\sum_{i=G+1}^{N} G_i \, p(G_i)}{\sum_{i=G+1}^{N} p(G_i)}$$

$$S_1 = \sum_{i=1}^{G} (M_1 - G_i)^2 \times p(G_i) \qquad S_2 = \sum_{i=G+1}^{N} (M_2 - G_i)^2 \times p(G_i)$$

$$W = (M - M_1)^2 + (M - M_2)^2$$

$$T = \min(H) = \min\left(\frac{(S_1 + S_2)}{W}\right)$$

* https://ui.adsabs.harvard.edu/link_gateway/1988SPIE.1001..261C/doi:10.1117/12.968961

Lung field Segmentation - Intensity-based Model

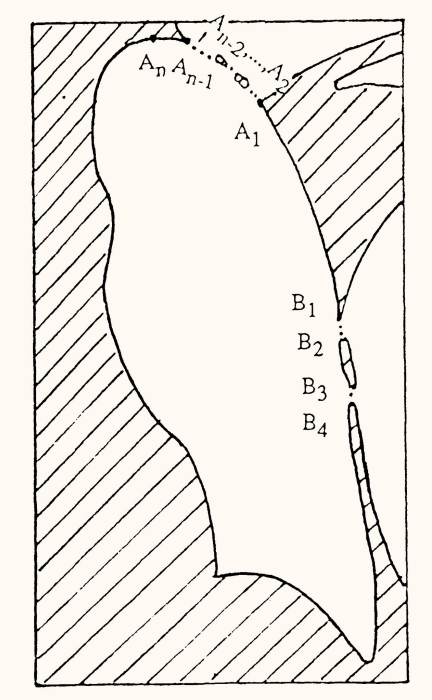

$$Y = a + bX + cX^2$$

$$\bar{Y} = a + b\bar{X} + c\bar{X^2}$$

$$\bar{XY} = a\bar{X} + b\bar{X^2} + c\bar{X^3}$$

$$\bar{X^2Y} = a\bar{X^2} + b\bar{X^3} + c\bar{X^4}$$

$$\bar{X^k} = \frac{1}{n}\sum_{i=1}^{k} X_i^k$$

$$\bar{X^kY} = \frac{1}{n}\sum_{i=1}^{k} X_i^k Y_i$$

* https://ui.adsabs.harvard.edu/link_gateway/1988SPIE.1001..261C/doi:10.1117/12.968961

Lung field Segmentation - DL Method

a) Original U-Net

b) All-Dropout

c) All-Convolutional

d) InvertedNet.

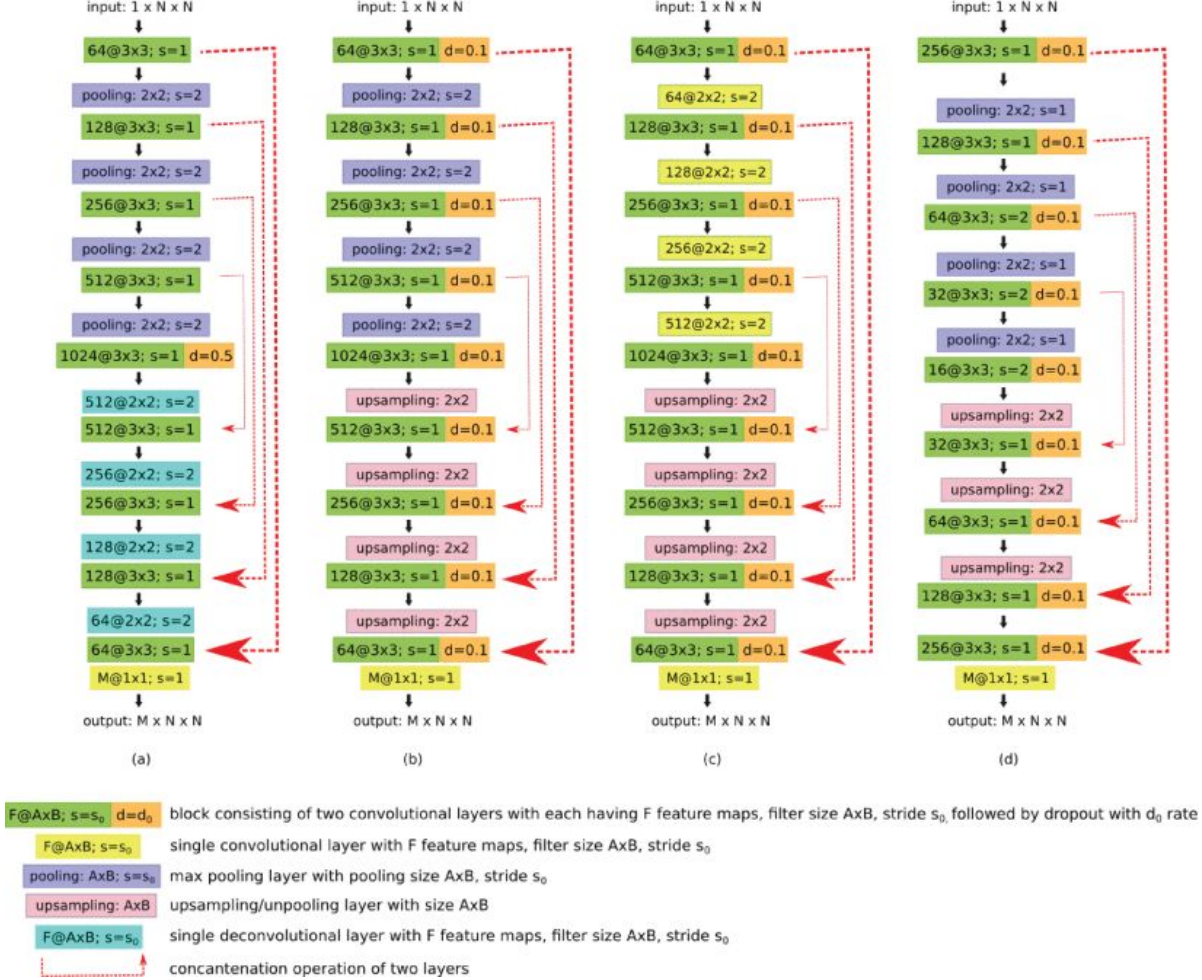

* https://ieeexplore.ieee.org/document/8302848

Data Driven Estimation of Covid-19 Prognosis

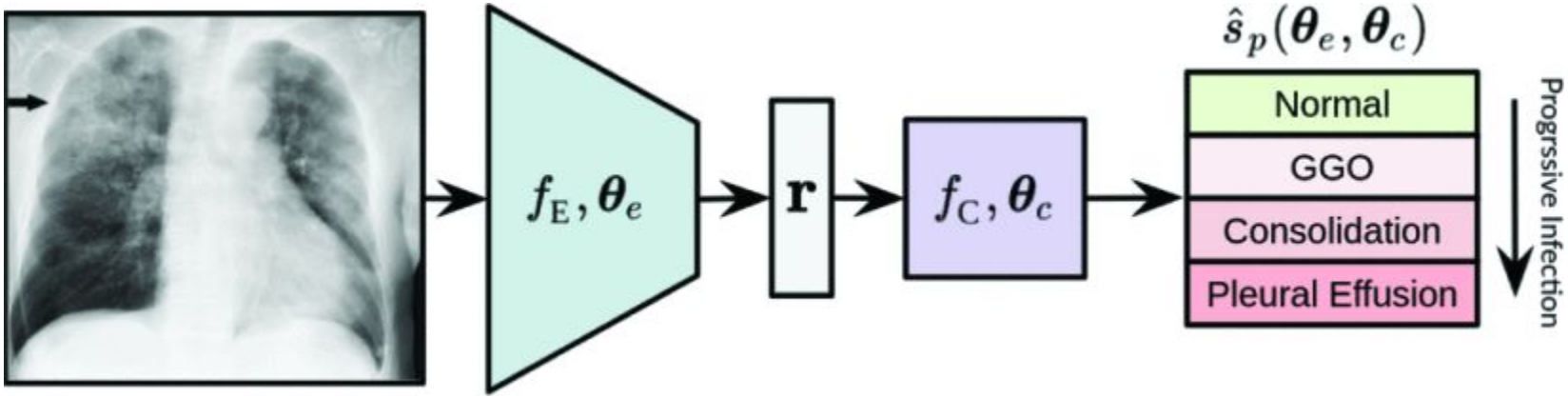

* https://ieeexplore.ieee.org/iel7/9761376/9761399/09761406.pdf

Data Driven Estimation of Covid-19 Prognosis

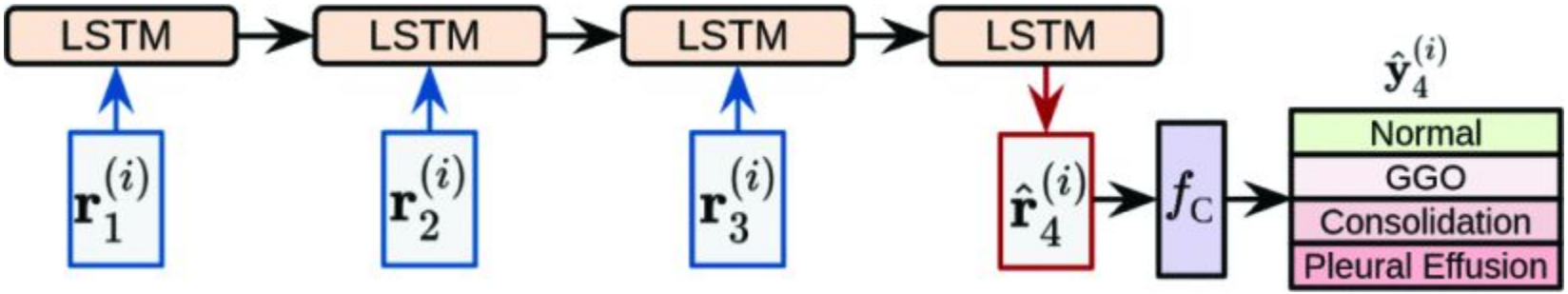

* https://ieeexplore.ieee.org/iel7/9761376/9761399/09761406.pdf

Additional Information - Image + Text

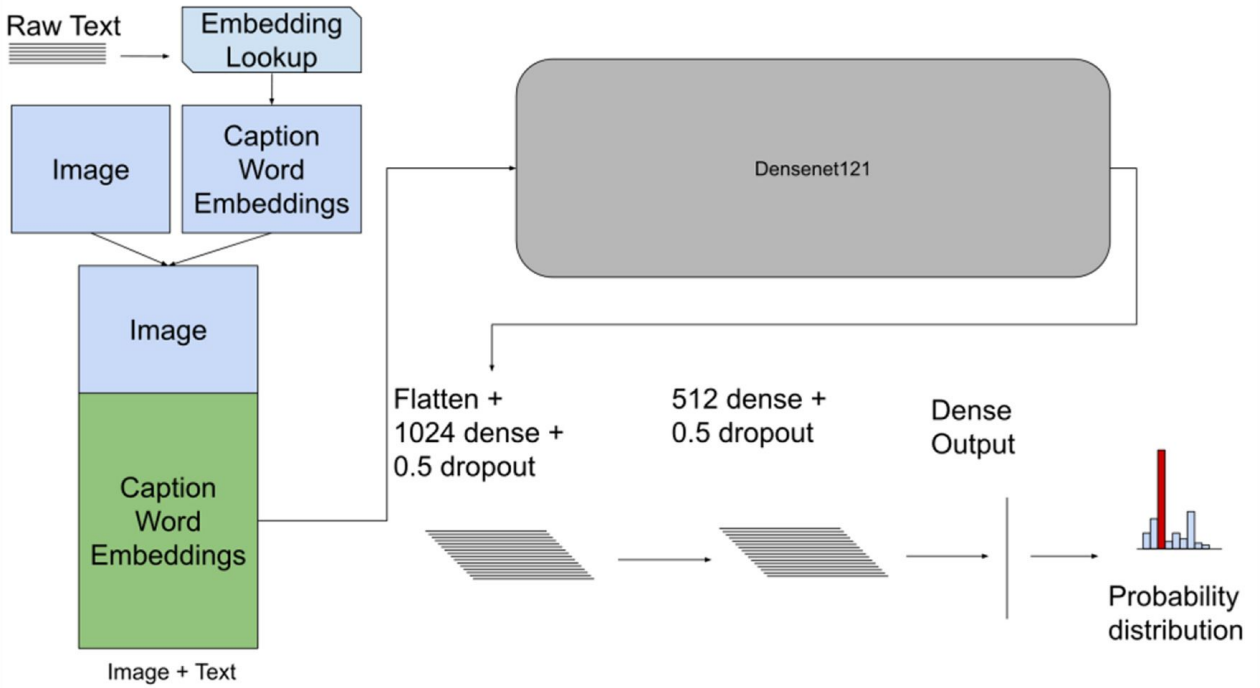

* https://doi.org/10.3389%2Ffdata.2020.00019

Additional Information - Image + Text

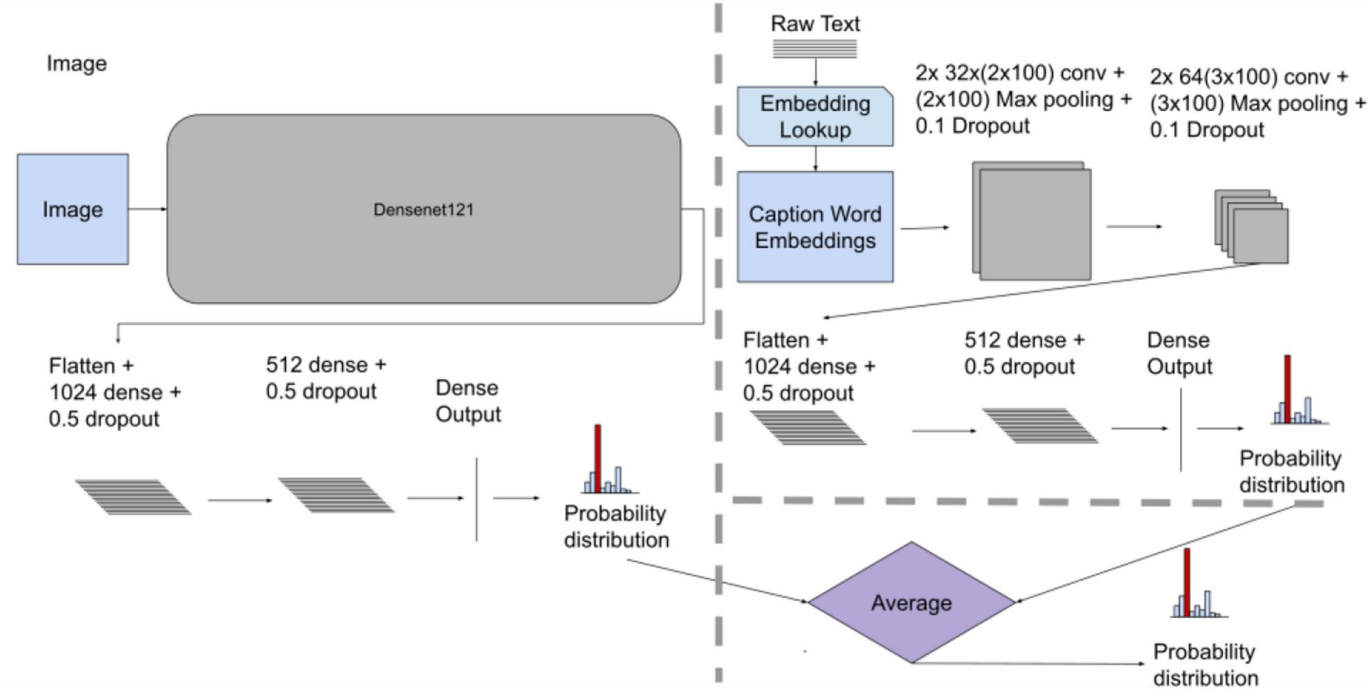

* https://doi.org/10.3389%2Ffdata.2020.00019

Additional Information - Image + Text

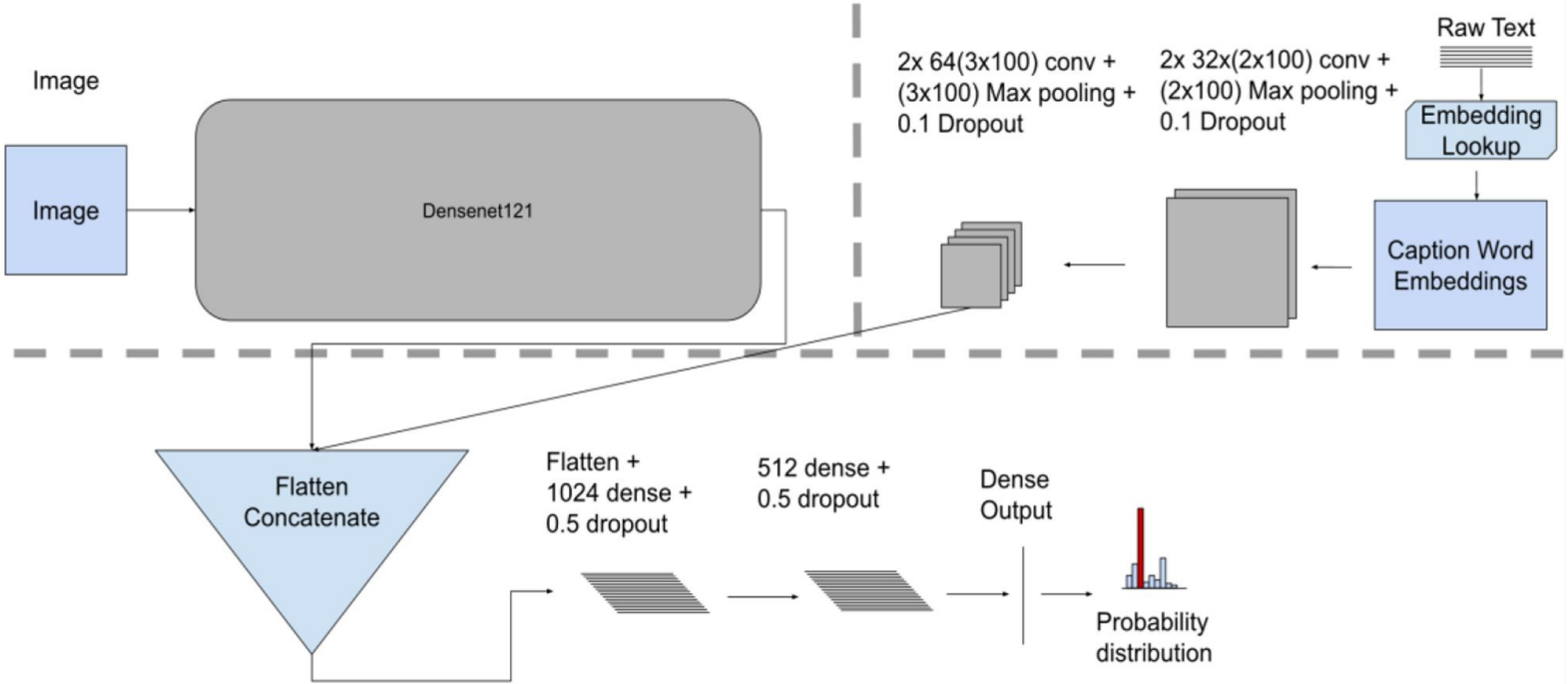

* https://doi.org/10.3389%2Ffdata.2020.00019

Additional Information -TIENET

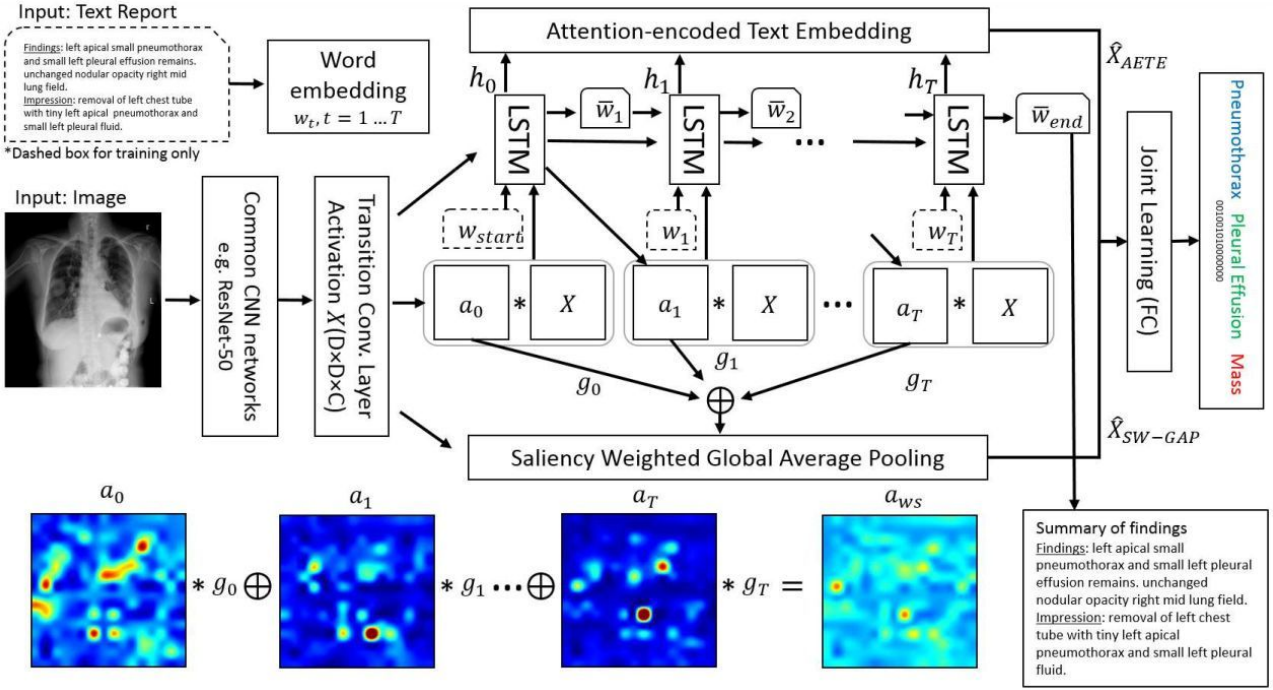

* https://ieeexplore.ieee.org/iel7/8576498/8578098/08579041.pdf

Additional Information - X-ray + ECG

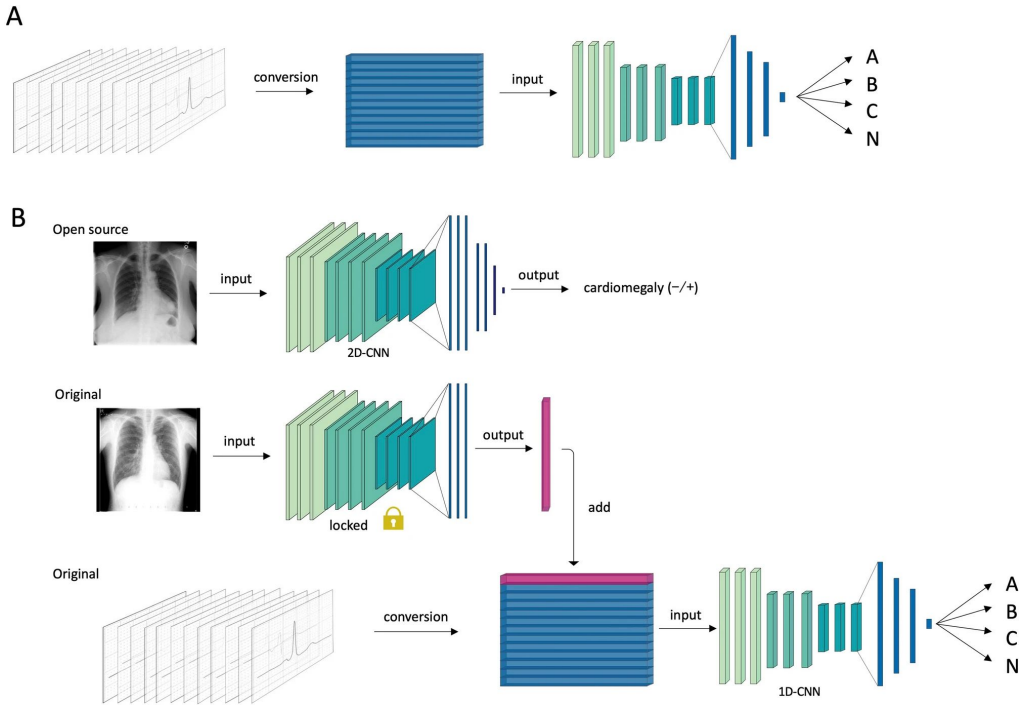

Overview of the deep learning architecture. (A) For the primary output, 206 ECGs were loaded into the convolutional neural network model and classified into four classifications (Group A, Group B, Group C, and Group N [normal class]). (B) For the secondary output, chest X-ray images from 1519 patients were used for pretraining, and the original chest X-ray images were compressed into a one-dimensional vector using the pretrained midlayer weights. The combined ECG and chest X-ray data were finally trained to classify the outputs. 2D-CNN indicates a two-dimensional convolutional neural network, and 1D-CNN indicates a one-dimensional convolutional neural network.

* https://www.nature.com/articles/s41598-021-87631-y

Chest X-ray Decomposition

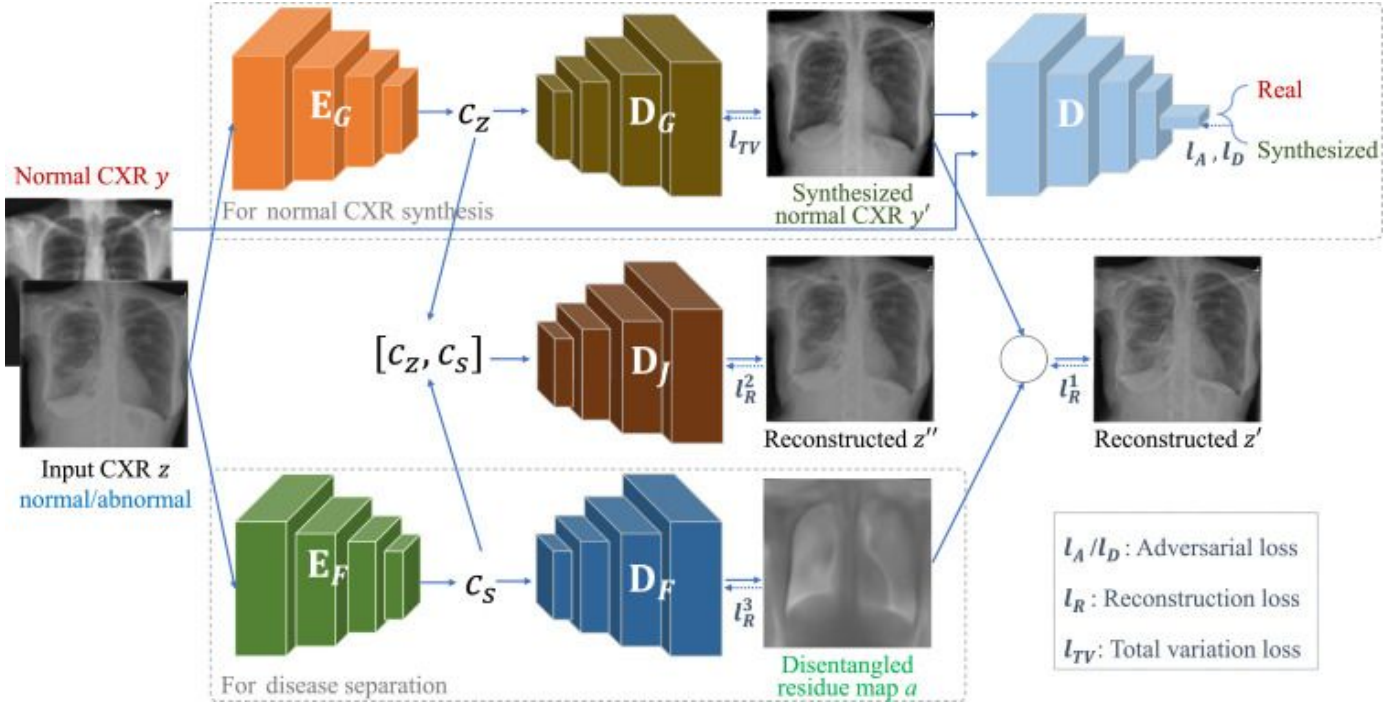

* https://www.sciencedirect.com/science/article/pii/S1361841520302036

Chest X-ray Decomposition

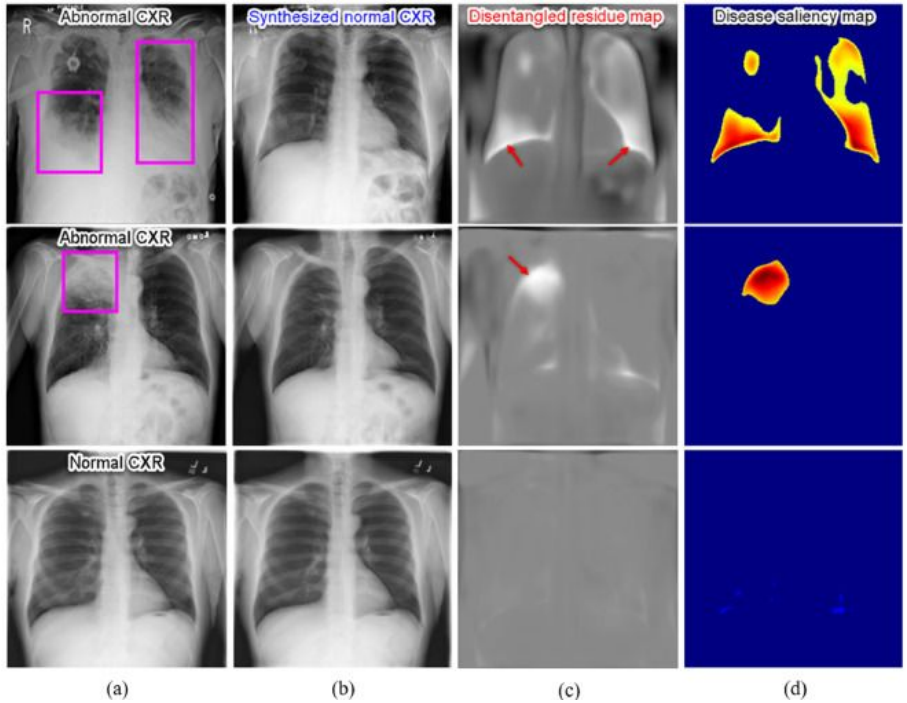

* https://www.sciencedirect.com/science/article/pii/S1361841520302036